Machine learning for materials discovery

Some example applications

Martin Uhrín

Computational Atomistic Methods and Machine Learning

Grenoble Alpes
Multidisciplinary Institute
In Artificial Intelligence

Machine learning from experiment

Ionic liquids to the rescue?

Energy density of Li-ion is 100-265 Wh kg^{-1}, contrast this with various metal-air chemistries:

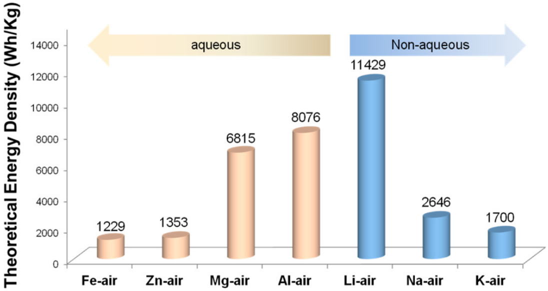

However, dendrite formation is one key problem hindering development of secondary (rechargeable) metal-air batteries.

Y. Li and J. Lu, "Metal–Air Batteries: Will They Be the Future Electrochemical Energy Storage Device of Choice?", ACS Energy Letters **2**, 1370–1377 (2017)

Ionic liquids to the rescue?

Energy density of Li-ion is 100-265 Wh kg^{-1}, contrast this with various metal-air chemistries:

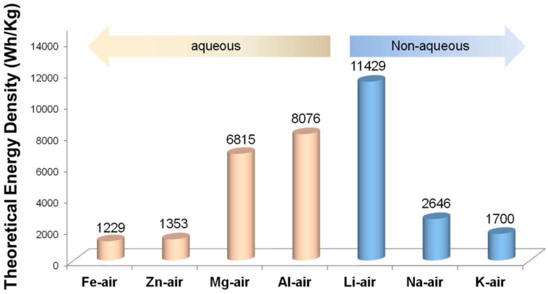

However, dendrite formation is one key problem hindering development of secondary (rechargeable) metal-air batteries.

Room Temperature Ionic Liquids (RTILs) all but eliminate dendrite formation

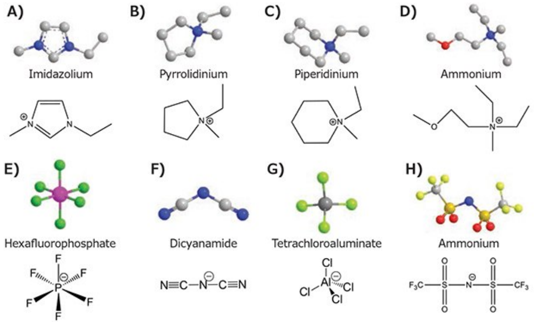

but suffer from high viscosity (and therefore low ionic conductivity).

Y. Li and J. Lu, "Metal–Air Batteries: Will They Be the Future Electrochemical Energy Storage Device of Choice?", ACS Energy Letters **2**, 1370–1377 (2017)

Machine learning ionic conductivity

Make the ansatz that the conductivity can be partitioned on a per-atom basis and parameterised as

$$\ln \frac{\epsilon}{R_0} = \sum_i^N \left[A_i + B_i \frac{1}{T} + C_i \left(\frac{1}{T} \right)^2 \right]$$

where A_i, B_i and C_i are fitting parameters.

Machine learning ionic conductivity

Make the ansatz that the conductivity can be partitioned on a per-atom basis and parameterised as

$$\ln \frac{\epsilon}{R_0} = \sum_i^N \left[A_i + B_i \frac{1}{T} + C_i \left(\frac{1}{T} \right)^2 \right]$$

where A_i, B_i and C_i are fitting parameters.

From experimental databases we get 4,093 data points, covering 310 unique ILs.
Split into training and test sets:

- Training: 260 ILs (3,351 data points)
- Test: 50 ILs (742 data point)

Machine learning ionic conductivity

Make the ansatz that the conductivity can be partitioned on a per-atom basis and parameterised as

$$\ln \frac{\epsilon}{R_0} = \sum_i^N \left[A_i + B_i \frac{1}{T} + C_i \left(\frac{1}{T} \right)^2 \right]$$

where A_i, B_i and C_i are fitting parameters.

From experimental databases we get 4,093 data points, covering 310 unique ILs.
Split into training and test sets:

- Training: 260 ILs (3,351 data points)
- Test: 50 ILs (742 data point)

Workflow

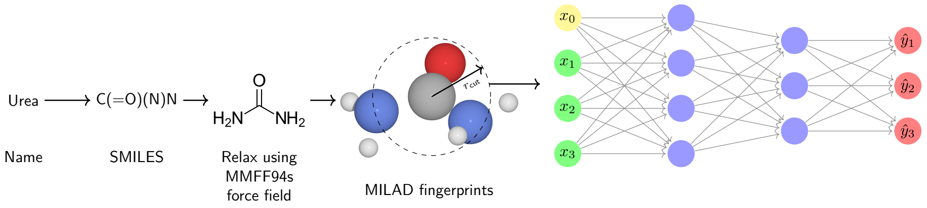

Predicting new ionic liquids

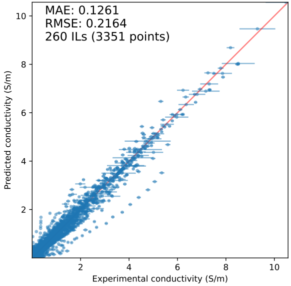

Training

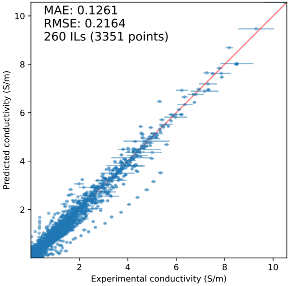

Validation

MU, A. S. Tygesen, T. Vegge, and J. H. Chang, *Predicting the conductivities of ionic liquids using machine learning*, in preparation

Predicting new ionic liquids

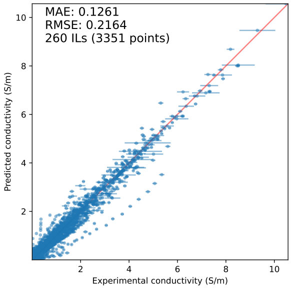

Training

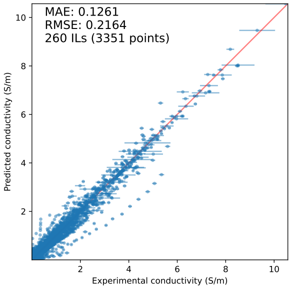

Validation

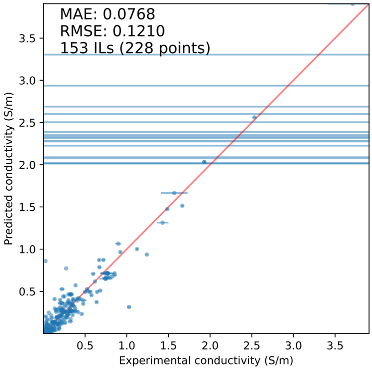

Novel of novel ILs

Anion	Cation	Conductivity (S/m)
cyanoiminomethylideneazanide	pyrrolidin-1-ium	4.39
cyanoiminomethylideneazanide	dimethyl(prop-2-enyl)azanium	3.30
nitrate	dimethyl(prop-2-enyl)azanium	2.93
cyanoiminomethylideneazanide	dimethyl(propyl)azanium	2.68
thiocyanate	pyrrolidin-1-ium	2.60
cyanoiminomethylideneazanide	1-ethyl-3-methyl-1,2-dihydroimidazol-1-ium	2.50

MU, A. S. Tygesen, T. Vegge, and J. H. Chang, *Predicting the conductivities of ionic liquids using machine learning*, in preparation

Machine learning from electronic structure

Accelerating electronic structure calculations

Local/semi-local XC functionals give poor description of electronic structure of strongly self-interacting materials.

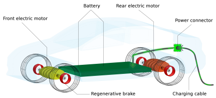

Batteries

Magnets for generators

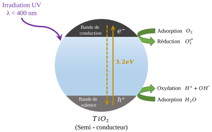

Photocatalysis

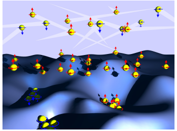

Spintronics

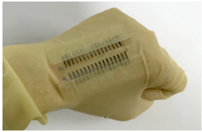

Thermoelectric devices

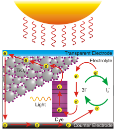

Dye-sensitised solar cells

Accelerating electronic structure calculations

Local/semi-local XC functionals give poor description of electronic structure of strongly self-interacting materials.

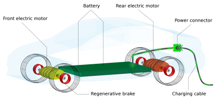

Batteries

Magnets for generators

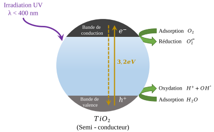

Photocatalysis

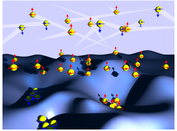

Spintronics

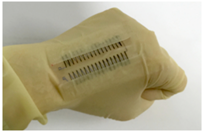

Thermoelectric devices

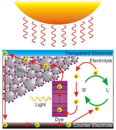

Dye-sensitised solar cells

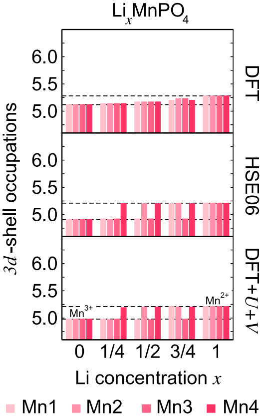

Hubbard corrections can help... but are computationally expensive.

Hubbard corrections

New total energy

$$E_{\mathsf{DFT}+U+V} = E_{\mathsf{DFT}} + E_{U+V}$$

where

$$E_{U+V} = \frac{1}{2}\sum_{I}\sum_{\sigma m m'} U^{I}\left(\delta_{mm'} - n^{II\sigma}_{mm'}\right) n^{II\sigma}_{m'm} - \frac{1}{2}\sum_{I}\sum^{*}_{J(J\neq I)}\sum_{\sigma m m'} V^{IJ} n^{IJ\sigma}_{mm'} n^{JI\sigma}_{m'm}\,.$$

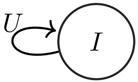

Favours localisation

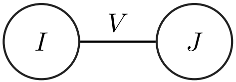

Favours hybridised states

V. Leiria Campo Jr and M. Cococcioni, "Extended DFT + U + V method with on-site and inter-site electronic interactions", Journal of Physics: Condensed Matter **22**, 055602 (2010)

Hubbard corrections

New total energy

$$E_{\mathsf{DFT}+U+V} = E_{\mathsf{DFT}} + E_{U+V}$$

where

$$E_{U+V} = \frac{1}{2}\sum_{I}\sum_{\sigma m m'} U^{I}\left(\delta_{mm'} - n^{II\sigma}_{mm'}\right) n^{II\sigma}_{m'm} - \frac{1}{2}\sum_{I}\sum_{J(J\neq I)}^{*}\sum_{\sigma m m'} V^{IJ} n^{IJ\sigma}_{mm'} n^{JI\sigma}_{m'm}\,.$$

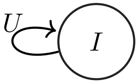

Favours localisation

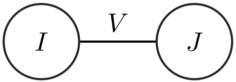

Favours hybridised states

Occupation matrices:

$$n^{IJ\sigma}_{mm'} = \sum_{v,\mathbf{k}} f^{\sigma}_{v,\mathbf{k}} \langle \psi^{\sigma}_{v,\mathbf{k}} | \phi^{J}_{m'} \rangle \langle \phi^{I}_{m} | \psi^{\sigma}_{v,\mathbf{k}} \rangle\,,$$

where

$$\phi^{I}_{m}(\mathbf{r}) \equiv \phi^{\gamma(I)}_{m}(\mathbf{r} - \mathbf{R}_I)$$

are localised orbitals on I^{th} atom.

V. Leiria Campo Jr and M. Cococcioni, "Extended DFT + U + V method with on-site and inter-site electronic interactions", Journal of Physics: Condensed Matter **22**, 055602 (2010)

Hubbard corrections

Correct DFT energy:

$$E_{\mathrm{DFT}+U+V} = E_{\mathrm{DFT}} + E_{U+V}$$

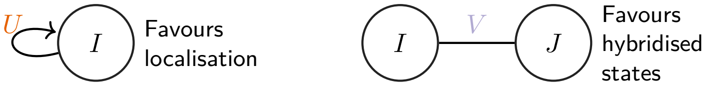

V. Leiria Campo Jr and M. Cococcioni, "Extended DFT + U + V method with on-site and inter-site electronic interactions", Journal of Physics: Condensed Matter **22**, 055602 (2010)

Hubbard corrections

Correct DFT energy:

$$E_{\mathsf{DFT}+U+V} = E_{\mathsf{DFT}} + E_{U+V}$$

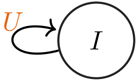

Favours localisation

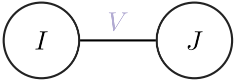

Favours hybridised states

Use U and V values calculated from applying generalised piece-wise linearity through linear-response theory.

Parameters free, but relatively expensive, ≈20xSCF

V. Leiria Campo Jr and M. Cococcioni, "Extended DFT + U + V method with on-site and inter-site electronic interactions", Journal of Physics: Condensed Matter **22**, 055602 (2010)

Computing Hubbard corrections

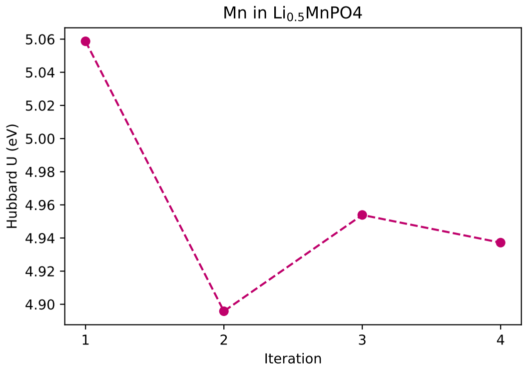

Protocol for self-consistent Hubbard U and V parameters

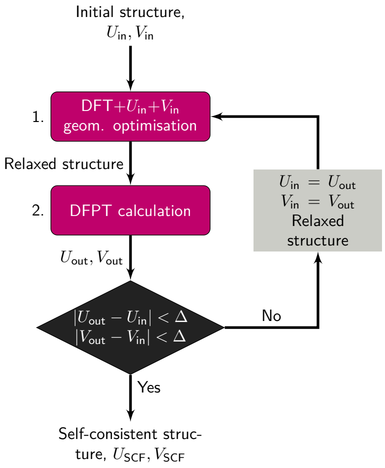

Computing Hubbard corrections

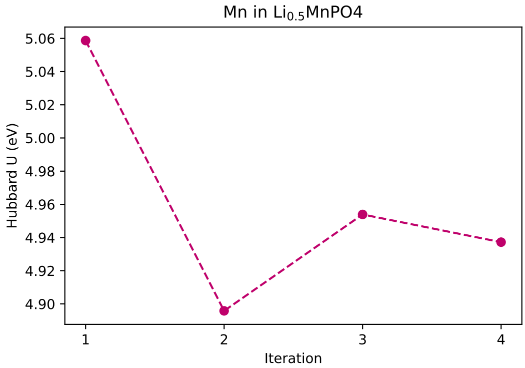

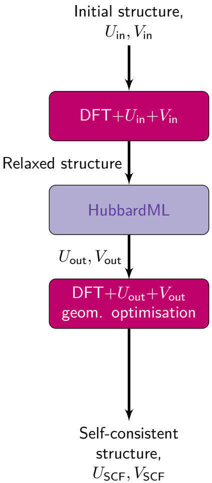

I. Timrov et al., "Hubbard parameters from density-functional perturbation theory", Physical Review B **98**, 085127 (2018); I. Timrov et al., "HP – A code for the calculation of Hubbard parameters using density-functional perturbation theory", Computer Physics Communications **279**, 108455 (2022)

The models

Hubbard U model

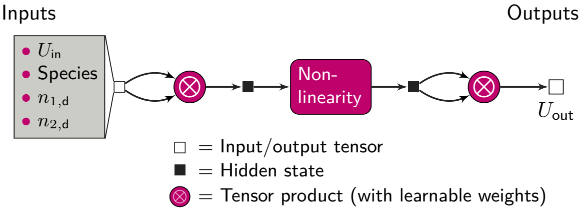

Hubbard V model

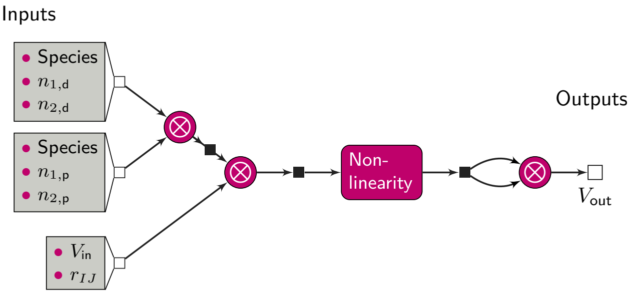

MU, A. Zadoks, L. Binci, N. Marzari, and I. Timrov, *Machine learning Hubbard parameters using equivariant neural networks and training data from linear-response theory*, in preparation.

Using data from[1] and Luca Binci:

- $Li_x FePO4$
- $Li_x MnPO4$
- $LiFe_{0.5}Mn_{0.5}PO4$
- Layered $Li_x CoO2$
- Layered $Li_x NiO2$
- Layered $Li_x MnO2$
- Layered $Li_x TiS2$
- $RNiO_3$

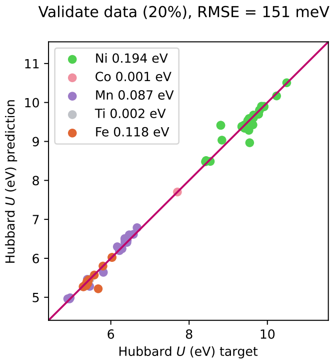

Self-consistent U

I. Timrov et al., "Self-consistent Hubbard parameters from density-functional perturbation theory in the ultrasoft and projector-augmented wave formulations", Physical Review B **103**, 45141 (2021)

MU, A. Zadoks, L. Binci, N. Marzari, and I. Timrov, *Machine learning Hubbard parameters using equivariant neural networks and training data from linear-response theory*, in preparation.

Using data from[1] and Luca Binci:

- Li_xFePO4
- Li_xMnPO4
- $LiFe_{0.5}Mn_{0.5}$PO4
- Layered Li_xCoO2
- Layered Li_xNiO2
- Layered Li_xMnO2
- Layered Li_xTiS2
- $RNiO_3$

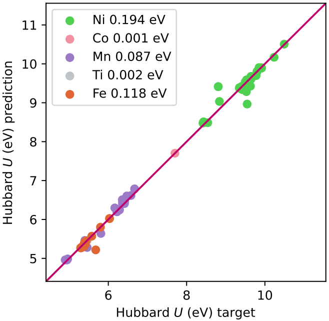

Self-consistent U

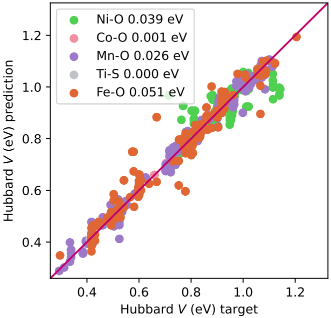

Self-consistent V

I. Timrov et al., "Self-consistent Hubbard parameters from density-functional perturbation theory in the ultrasoft and projector-augmented wave formulations", Physical Review B **103**, 45141 (2021)

MU, A. Zadoks, L. Binci, N. Marzari, and I. Timrov, *Machine learning Hubbard parameters using equivariant neural networks and training data from linear-response theory*, in preparation.

Different occupations - Hubbard U

x in Li_x\{Fe,Mn\}PO_4	0	0.25	0.5	0.75	1
Mn	16	32	16	16	16
Fe	16	20	16	8	12

Different occupations - Hubbard U

x in $Li_x\{Fe,Mn\}PO_4$	0	0.25	0.5	0.75	1
Mn	16	32	16	16	16
Fe	16	20	16	8	12

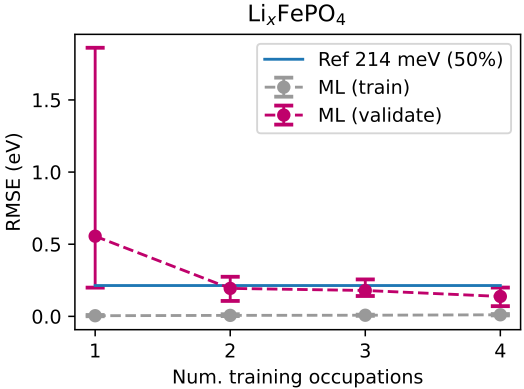

Different occupations - Hubbard U

Mn	16	32	16	16	16
Fe	16	20	16	8	12
x in $Li_x\{Fe,Mn\}PO_4$	0	0.25	0.5	0.75	1

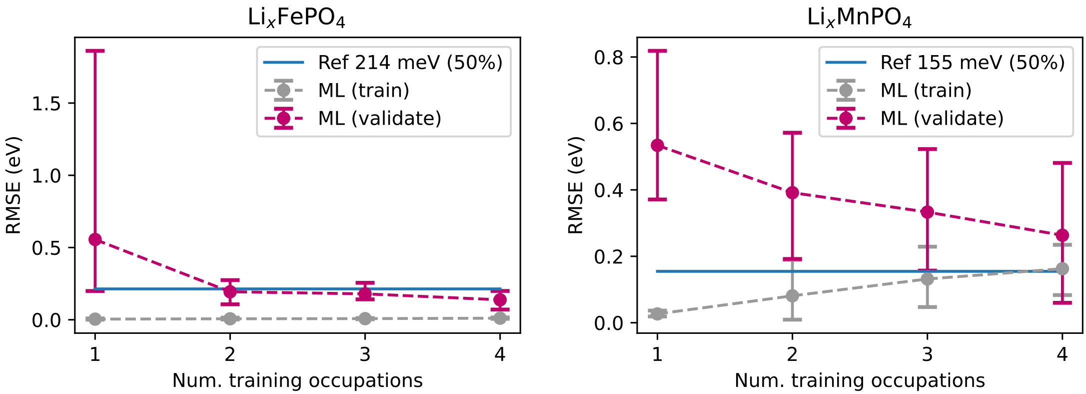

Generative modelling for modelling amorphous materials

Motivation

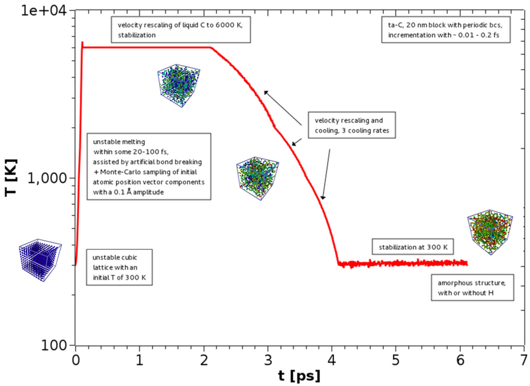

Timo Hakala, Kenneth Holmberg and Anssi Laukkanen. Lubricants. 9. 30. (2021).

Motivation

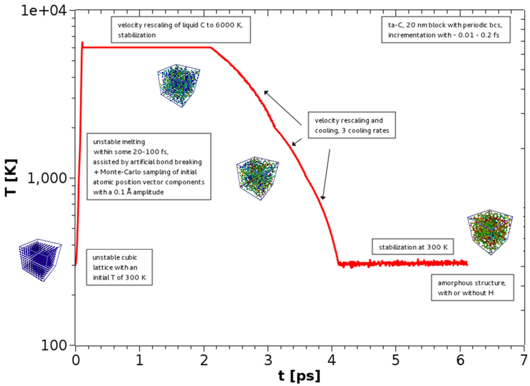

Given an example structure(s), can we teach a generative machine learning model to generate novel examples, bypassing the need for further molecular dynamics?

Timo Hakala, Kenneth Holmberg and Anssi Laukkanen. Lubricants. 9. 30. (2021).

The Variational Autoencoder

The autoencoder

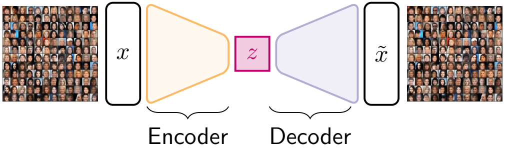

$$\mathcal{L} = (x - \tilde{x})^2$$

The Variational Autoencoder

The autoencoder

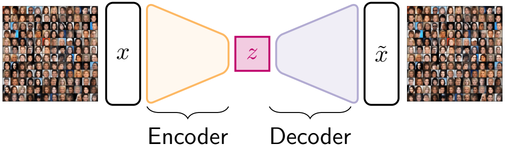

$$\mathcal{L} = (x - \tilde{x})^2$$

The *variational* autoencoder

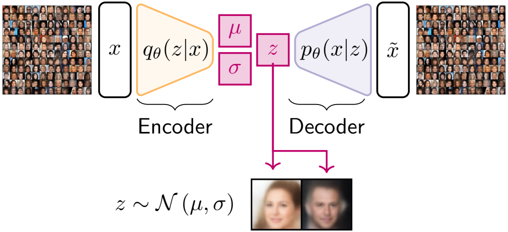

$$z \sim \mathcal{N}(\mu, \sigma)$$

$$\mathcal{L} = (x - \tilde{x})^2 + \sum_j KL(q_j(z|x)||p(z))$$

The Variational Autoencoder

The autoencoder

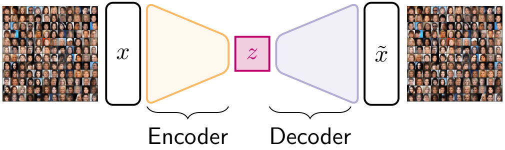

$$\mathcal{L} = (x - \tilde{x})^2$$

The *variational* autoencoder

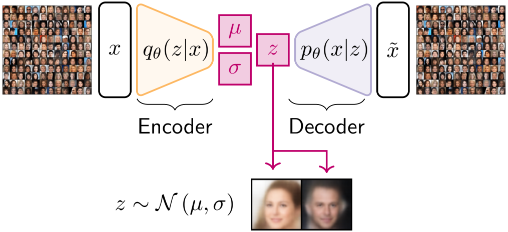

$$\mathcal{L} = (x - \tilde{x})^2 + \sum_j KL(q_j(z|x)||p(z))$$

Kullback-Leibler divergence

$$D_{\mathrm{KL}}(P \parallel Q) = \int_{-\infty}^{\infty} p(x) \ \log\left(\frac{p(x)}{q(x)}\right) \ \mathrm{d}x$$

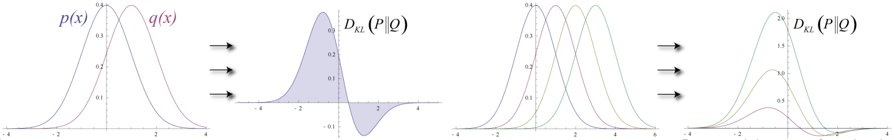

Variational autoencoder for atomic motifs

Training

1 For each atom in unit cell, extract local atomic environment up to r_{cut}. Keeps closest n atoms

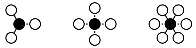

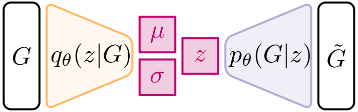

minimise
$\mathcal{L} = (G - \tilde{G})^2 + \sum_j KL(q_j(z|G)||p(z))$

Variational autoencoder for atomic motifs

Training

1. For each atom in unit cell, extract local atomic environment up to r_{cut}. Keeps closest n atoms

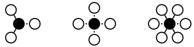

2. Calculate Gram matrix $x^i \cdot x^j$, keep upper triangular part, $j \geq i$

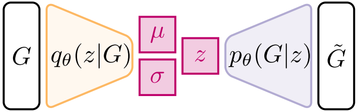

minimise

$$\mathcal{L} = (G - \tilde{G})^2 + \sum_j KL(q_j(z|G)||p(z))$$

Variational autoencoder for atomic motifs

Training

1. For each atom in unit cell, extract local atomic environment up to r_{cut}. Keeps closest n atoms

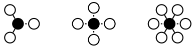

2. Calculate Gram matrix $x^i \cdot x^j$, keep upper triangular part, $j \geq i$
3. Generate permutation copies of atom labels i (data augmentation) e.g. $[1, 2, 3], [1, 3, 2], [2, 1, 3]$, etc

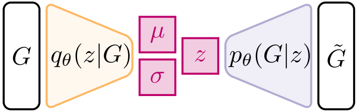

minimise

$$\mathcal{L} = (G - \tilde{G})^2 + \sum_j KL(q_j(z|G)||p(z))$$

Variational autoencoder for atomic motifs

Training

1. For each atom in unit cell, extract local atomic environment up to r_{cut}. Keeps closest n atoms

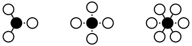

2. Calculate Gram matrix $x^i \cdot x^j$, keep upper triangular part, $j \geq i$
3. Generate permutation copies of atom labels i (data augmentation) e.g. $[1, 2, 3], [1, 3, 2], [2, 1, 3]$, etc
4. Train VAE using gradient-based optimisation

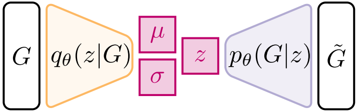

minimise
$\mathcal{L} = (G - \tilde{G})^2 + \sum_j KL(q_j(z|G)||p(z))$

Variational autoencoder for atomic motifs

$$E = \begin{bmatrix} r_1 \\ r_2 \\ \vdots \\ r_N \end{bmatrix} = \begin{bmatrix} x_1 & y_1 & z_1 \\ x_2 & y_2 & z_2 \\ \vdots & \vdots & \vdots \\ x_N & y_N & z_N \end{bmatrix}$$

Initial atomic environment

Loss function on the invariants: $\|G - G'\|^2 + D_{KL}$

input

$$G = \begin{bmatrix} \langle \mathbf{r}_1, \mathbf{r}_1 \rangle & \langle \mathbf{r}_1, \mathbf{r}_2 \rangle & \dots & \langle \mathbf{r}_1, \mathbf{r}_N \rangle \\ \langle \mathbf{r}_1, \mathbf{r}_1 \rangle & \langle \mathbf{r}_1, \mathbf{r}_2 \rangle & \dots & \langle \mathbf{r}_1, \mathbf{r}_N \rangle \\ \vdots & \vdots & \ddots & \vdots \\ \langle \mathbf{r}_N, \mathbf{r}_1 \rangle & \langle \mathbf{r}_N, \mathbf{r}_2 \rangle & \dots & \langle \mathbf{r}_N, \mathbf{r}_N \rangle \end{bmatrix}$$

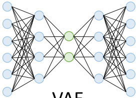

VAE

reconstructed

$$\begin{bmatrix} \langle \mathbf{r'}_1, \mathbf{r'}_1 \rangle & \langle \mathbf{r'}_1, \mathbf{r'}_2 \rangle & \dots & \langle \mathbf{r'}_1, \mathbf{r'}_N \rangle \\ \langle \mathbf{r'}_1, \mathbf{r'}_1 \rangle & \langle \mathbf{r'}_1, \mathbf{r'}_2 \rangle & \dots & \langle \mathbf{r'}_1, \mathbf{r'}_N \rangle \\ \vdots & \vdots & \ddots & \vdots \\ \langle \mathbf{r'}_N, \mathbf{r'}_1 \rangle & \langle \mathbf{r'}_N, \mathbf{r'}_2 \rangle & \dots & \langle \mathbf{r'}_N, \mathbf{r'}_N \rangle \end{bmatrix} = G'$$

SVD

$$\begin{bmatrix} x'_1 & y'_1 & z'_1 \\ x'_2 & y'_2 & z'_2 \\ \vdots & \vdots & \vdots \\ x'_N & y'_N & z'_N \end{bmatrix} = \begin{bmatrix} r'_1 \\ r'_2 \\ \vdots \\ r'_N \end{bmatrix} = E'$$

Reconstructed atomic environment

The problem with invariants space

$$\begin{bmatrix} x_1 & y_1 & z_1 \\ x_2 & y_2 & z_2 \\ & \vdots & \\ x_N & y_N & z_N \end{bmatrix} \quad \text{vs} \quad \begin{bmatrix} x^1 \cdot x^1 & \cdots & x^1 \cdot x^N \\ \vdots & \ddots & \vdots \\ x^N \cdot x^1 & \cdots & x^N \cdot x^N \end{bmatrix}$$

$$3N(-6) \quad \text{DoFs} \quad \text{vs} \quad \frac{N(N+1)}{2} \quad \text{DoFs}$$

The problem with invariants space

$$\begin{bmatrix} x_1 & y_1 & z_1 \\ x_2 & y_2 & z_2 \\ & \vdots & \\ x_N & y_N & z_N \end{bmatrix} \quad \text{vs} \quad \begin{bmatrix} x^1 \cdot x^1 & \cdots & x^1 \cdot x^N \\ \vdots & \ddots & \vdots \\ x^N \cdot x^1 & \cdots & x^N \cdot x^N \end{bmatrix}$$

$$3N(-6) \quad \text{DoFs} \quad \text{vs} \quad \frac{N(N+1)}{2} \quad \text{DoFs}$$

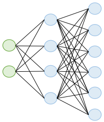

Decoder

→ $\tilde{\boldsymbol{\Phi}}$ →

Generated fingerprints

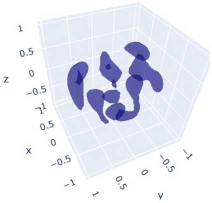

$\tilde{f}(r_i, \ldots)$

Density grid

The problem with invariants space

$$\begin{bmatrix} x_1 & y_1 & z_1 \\ x_2 & y_2 & z_2 \\ & \vdots & \\ x_N & y_N & z_N \end{bmatrix} \quad \text{vs} \quad \begin{bmatrix} x^1 \cdot x^1 & \cdots & x^1 \cdot x^N \\ \vdots & \ddots & \vdots \\ x^N \cdot x^1 & \cdots & x^N \cdot x^N \end{bmatrix}$$

$$3N(-6) \quad \text{DoFs} \quad \text{vs} \quad \frac{N(N+1)}{2} \quad \text{DoFs}$$

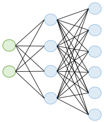

Decoder

$\rightarrow \tilde{\boldsymbol{\Phi}} \rightarrow$

Generated fingerprints

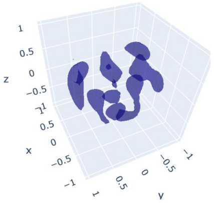

$\tilde{f}(r_i, \ldots)$

Density grid

The solution: synchronisation

X X’

The problem with invariants space

$$\begin{bmatrix} x_1 & y_1 & z_1 \\ x_2 & y_2 & z_2 \\ & \vdots & \\ x_N & y_N & z_N \end{bmatrix} \quad \text{vs} \quad \begin{bmatrix} x^1 \cdot x^1 & \cdots & x^1 \cdot x^N \\ \vdots & \ddots & \vdots \\ x^N \cdot x^1 & \cdots & x^N \cdot x^N \end{bmatrix}$$

$$3N(-6) \quad \text{DoFs} \quad \text{vs} \quad \frac{N(N+1)}{2} \quad \text{DoFs}$$

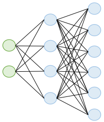

Decoder → $\tilde{\boldsymbol{\Phi}}$ →

Generated fingerprints

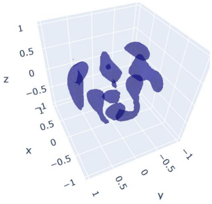

$\tilde{f}(r_i, \dots)$

Density grid

The solution: synchronisation

X X'

We know

$$X = QX'$$

with some rotation matrix Q.
We can solve for this using:

$$\min_{Q} \|X - QX'\|_F$$

Training and generating

Training

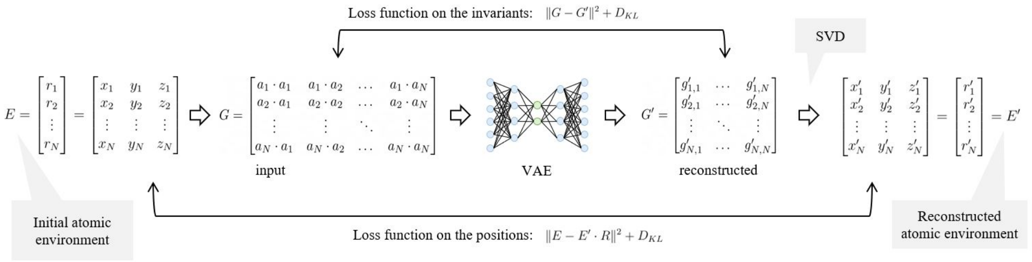

Training and generating

Training

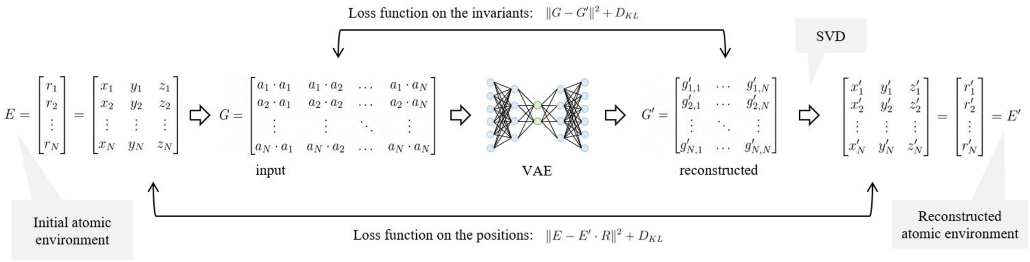

Generating

Draw n_Z samples from $\mathcal{N}(0, 1)$

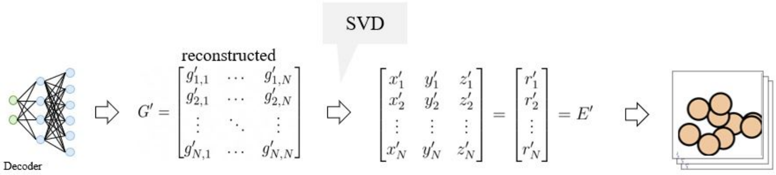

Variational autoencoder for atomic motifs

All tests performed in amorphous Si, 512 atom unit cells generated using ML potential trained on DFT[1].

- Radial cutoff: 4 Å
- 8 atoms per environment
- latent space: 8 neurons (compared to $3n - 6 = 18$ DoFs)
- Encoder architecture 36-28-18-8 with tanh activations

Data normalisation

- $G'_{ii} = (G_{ii} - \mu_{\text{diag}})/\sigma_{\text{diag}}$
- $G'_{ij} = (G_{ij} - \mu_{\text{off-diag}})/\sigma_{\text{off-diag}}, i < j$

V. L. Deringer et al., "Realistic Atomistic Structure of Amorphous Silicon from Machine-Learning-Driven Molecular Dynamics", Journal of Physical Chemistry Letters **9**, 2879–2885 (2018)

Example generated environments

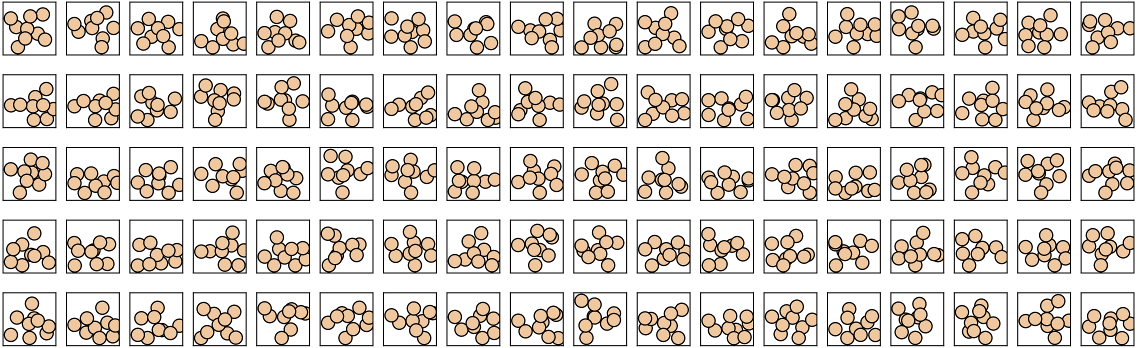

Model performance

Training reconstruction

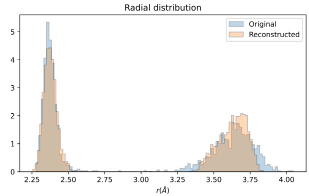

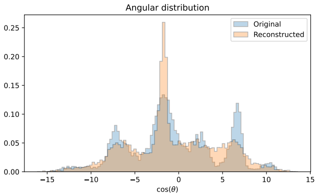

Model performance

Training reconstruction

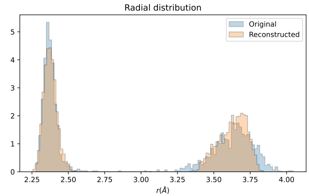

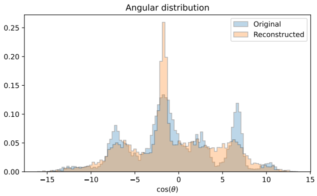

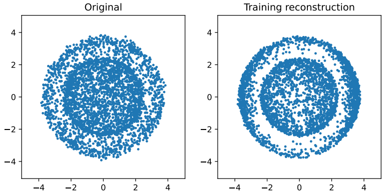

Model performance

Training reconstruction

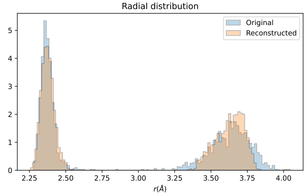

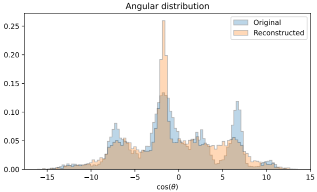

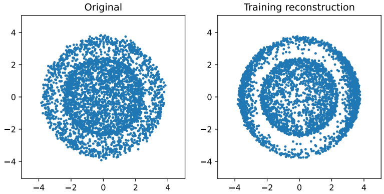

Generated samples

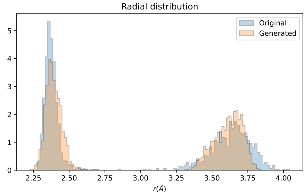

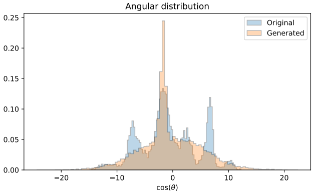

Model performance

Training reconstruction

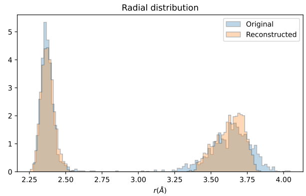

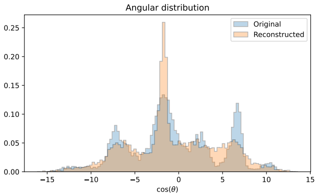

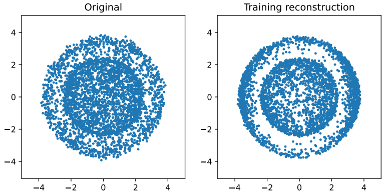

Generated samples

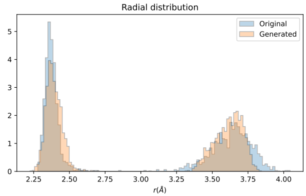

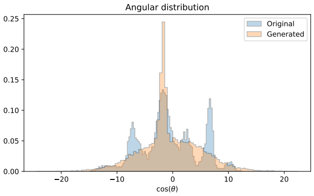

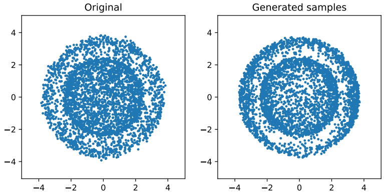

Model performance

Training reconstruction

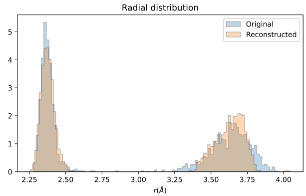

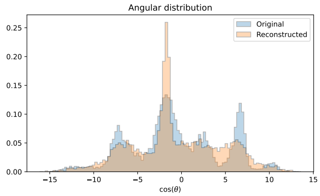

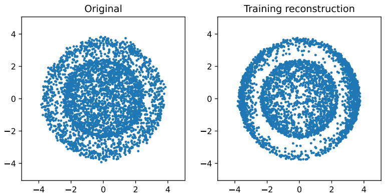

Generated samples

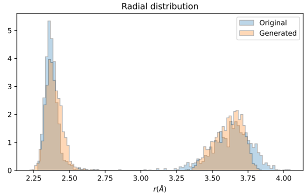

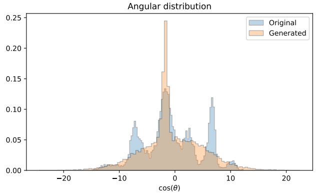

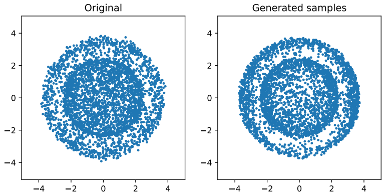

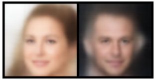

Interpolating between motifs

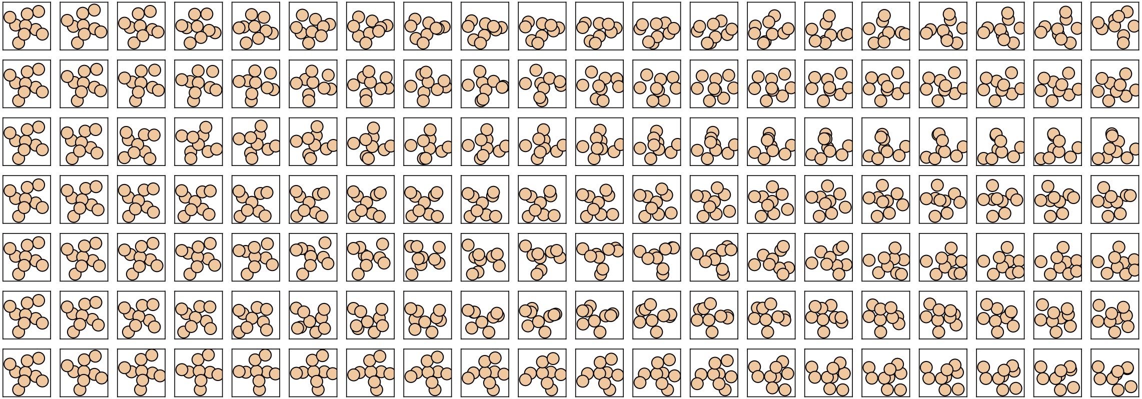

Interpolating between motifs

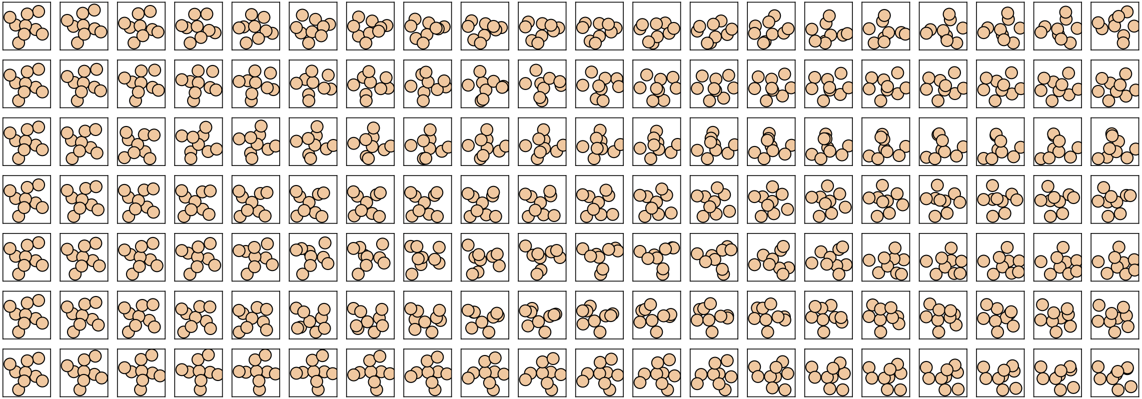

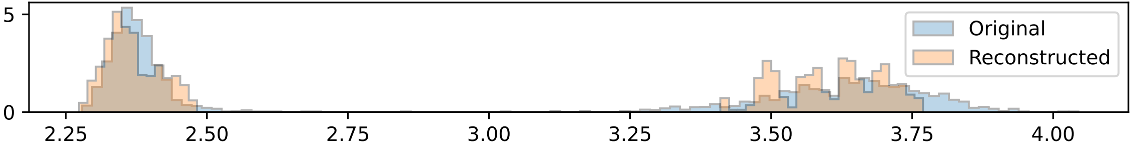

Inpainting

Atom infilling: Building complete unit cells

Image inpainting

Chan2005a

Atom infilling: Building complete unit cells

Image inpainting

Environment infilling

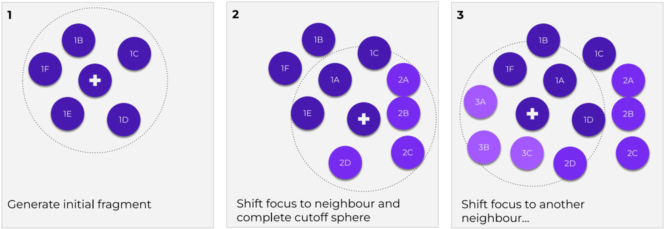

Chan2005a

Atom infilling

Setup

- Calculate initial Gram matrix with known atoms, fill in rest with noise G^I
- Project into latent space $z^I = f_{\text{encode}}(G^I)$

Atom infilling

Setup

- Calculate initial Gram matrix with known atoms, fill in rest with noise G^I
- Project into latent space $z^I = f_{\text{encode}}(G^I)$

Objective function

$$\min_z \| f_{\text{decode}}(z) - G \circ f_{\text{decode}}(z) \|^2$$

i.e. find point that lies on latent space manifold *and* where known atoms are in their original positions.

Atom infilling results

Fixed atoms: 7

Fixed atoms: 6

Fixed atoms: 5

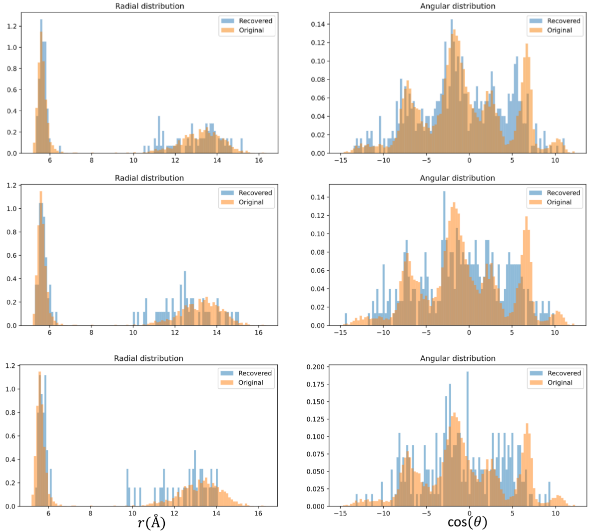

Atom infilling results